Continuous analysis of waveform relaxation for heterogeneous heat equations

Philipp Birken[0000−0002−6706−3634] and Martin J. Gander[0000−0001−8450−9223] and Niklas Kotarsky[0009−0001−5135−3776]

1 Introduction

We consider the coupling of time dependent partial differential equations (PDEs) across an interface. This can be used to describe the exchange of heat or of forces between different domains. It plays an important role in a multitude of applications, e.g. flutter of airplanes (forces), gas quenching (heat) or ocean-atmosphere interaction in climate modeling (both).

It is desirable to reuse existing codes for the subproblems, since these represent long term development work. This is called a partitioned coupling approach. Within this approach, the two submodels interact by exchanging boundary conditions at the interface. A specific choice of boundary conditions leads, e.g., to a Dirichlet-Neumann method or a Robin-Robin method. Here, our focus is on the Dirichlet-Neumann variant, since most existing solvers support these boundary conditions. Our general aim is a partitioned method that is high order, allows for different and adaptive time steps in the separate models, parallel execution, makes efficient use of hardware resources, is robust, and contains fast inner solvers. The major candidates to achieve such a method are so called *Waveform Relaxation* (WR) methods. These solve two coupled ODEs by iterating between solving them separately, using data from the other. Their convergence behavior can be improved using relaxation, with a problem dependent optimized relaxation parameter.

To design and effectively use such methods, e.g. to decide which submodel should use the Dirichlet transmission condition, it is important to have analytical error estimates. Based on existing results for the continuous case, we derive new such error

Niklas Kotarsky
Centre for Mathematical Sciences, Lund University e-mail: niklas.kotarsky@math.lu.se

Philipp Birken
Centre for Mathematical Sciences, Lund University e-mail: philipp.birken@math.lu.se

Martin J. Gander
Section de Mathématiques, Université de Genève, e-mail: martin.gander@unige.ch

estimates for two coupled heterogeneous linear heat equations in 1D, which we consider to be a minimal example of relevance, namely

$$\begin{aligned}
\alpha_1 \partial_t u_1 - \lambda_1 \partial_{xx} u_1 &= 0 \text{ on } [-a,0]\times[0,T],\\
\alpha_2 \partial_t u_2 - \lambda_2 \partial_{xx} u_2 &= 0 \text{ on } [0,b]\times[0,T],\\
u_1(-a,t) &= 0 \text{ in } [0,T],\\
u_1(0,t) &= u_2(0,t) \text{ in } [0,T],\\
u_1(b,t) &= 0 \text{ in } [0,T],\\
u_1(x,0) &= u_0(x) \text{ on } [-a,0],\\
u_2(x,0) &= u_0(x) \text{ on } [0,b],\\
-\lambda_1 \partial_n u_1(0,t) &= \lambda_2 \partial_n u_2(0,t) \text{ in } [0,T].
\end{aligned} \tag{1}$$

Here, u_i is the temperature, λ_i the heat conductivity and α_i the product of density and specific heat conductivity on domain Ω_i, and ∂_n denotes the normal derivative. To solve problem (1) iteratively, we make use of Dirichlet-Neumann Waveform Relaxation (DNWR). At the continuous level, we can write the $(k+1)^{\text{th}}$ iteration as

$$\begin{aligned}
\alpha_1 \partial_t u_1^{k+1} - \lambda_1 \partial_{xx} u_1^{k+1} &= 0 \text{ on } [-a,0]\times[0,T],\\
u_1^{k+1}(-a,t) &= 0 \text{ on } [0,T],\\
u_1^{k+1}(0,t) &= h^k \text{ on } [0,T],\\
u_1^{k+1}(x,0) &= u_0(x) \text{ on } [-a,0],\\
\alpha_2 \partial_t u_2^{k+1} - \lambda_2 \partial_{xx} u_2^{k+1} &= 0 \text{ on } [0,b]\times[0,T],\\
u_2^{k}(b,t) &= 0 \text{ on } [0,T],\\
-\lambda_1 \partial_n u_1^{k+1}(0,t) &= \lambda_2 \partial_n u_2^{k+1}(0,t) \text{ on } [0,T],\\
u_2^{k+1}(x,0) &= u_0(x) \text{ on } [0,b],
\end{aligned} \tag{2}$$

combined with the relaxation step

$$h^{k+1} = \theta u_2^{k+1}(x,t)\mid_{x=0} + (1-\theta)h^k, \tag{3}$$

where $\theta \in [0,1]$ is a relaxation parameter. To start the iteration, an initial guess has to be provided for h^0, which in practice is often chosen as the constant $u_0(0)$.

In [3], the DNWR iteration (2)-(3) was analyzed with all material parameters equal to one. The analysis is based on a Laplace transform in time, which results in two boundary value problems that can be solved in closed form, giving an update formula for the interface values in Laplace space. An optimal relaxation parameter $\theta = \frac{1}{2}$ was determined, and error estimates were obtained in the supremum norm in time, which show a dependence on the domain size.

In [4, 1], variable heat conductivity was considered for the case $\alpha_1 = \alpha_2 = 1$. The authors used a Fourier transform in time, and obtained that the DNWR iteration without relaxation has a convergence factor of $\sqrt{\lambda_1/\lambda_2}$ on infinite domains.

2 Convergence Analysis of the heterogeneous DNWR

To analyze the convergence behavior of the DNWR iteration (2)-(3), we study the error equations, where all boundary and initial data except for the initial guess h^0 are set to 0. Laplace transforming the error equations in time yields

$$\begin{aligned}
\alpha_1 s\hat{u}_1^{k+1} - \lambda_1\partial_{xx}\hat{u}_1^{k+1} &= 0 \text{ on } x \in [-a,0] \text{ and } s \in \mathbb{C},\\
\hat{u}_1^{k+1}(-a,s) &= 0 \text{ on } s \in \mathbb{C},\\
\hat{u}_1^{k+1}(0,s) &= \hat{h}^k \text{ on } s \in \mathbb{C},\\
\alpha_2 s\hat{u}_2^{k+1} - \lambda_2\partial_{xx}\hat{u}_2^{k+1} &= 0 \text{ on } x \in [-a,0] \text{ and } s \in \mathbb{C},\\
\hat{u}_1^{k}(b,s) &= 0 \text{ on } s \in \mathbb{C},\\
-\lambda_1\partial_n\hat{u}_1^{k+1}(0,s) &= \lambda_2\partial_n\hat{u}_2^{k+1}(0,s) \text{ on } s \in \mathbb{C},
\end{aligned} \tag{4}$$

where s is the Laplace variable. This is combined with the transformed update

$$\hat{h}^{k+1} = \theta\hat{u}_2^{k+1}(x,t)\mid_{x=0} + (1-\theta)\hat{h}^k. \tag{5}$$

Solving both sub problems in the transformed DNWR iteration (4) yields

$$\begin{aligned}
\hat{u}_1^{k+1} &= \frac{\sinh\left(\sqrt{\alpha_1/\lambda_1}(x+a)\sqrt{s}\right)}{\sinh\left(\sqrt{\alpha_1/\lambda_1}a\sqrt{s}\right)}\hat{h}^k,\\
\hat{u}_2^{k+1} &= -\sqrt{\frac{\alpha_1\lambda_1}{\alpha_2\lambda_2}}\frac{\coth\left(\sqrt{\alpha_1/\lambda_1}a\sqrt{s}\right)}{\cosh\left(\sqrt{\alpha_2/\lambda_2}b\sqrt{s}\right)}\sinh\left(\sqrt{\alpha_2/\lambda_2}(x-b)\sqrt{s}\right)\hat{h}^k,\\
\hat{h}^{k+1} &= \left((1-\theta) - \theta\sqrt{\frac{\alpha_1\lambda_1}{\alpha_2\lambda_2}}\coth\left(\sqrt{\alpha_1/\lambda_1}a\sqrt{s}\right)\tanh\left(\sqrt{\alpha_2/\lambda_2}b\sqrt{s}\right)\right)\hat{h}^k.
\end{aligned}$$

In [3], both a linear and a super-linear convergence estimate were derived for the case where $\alpha_1 = \lambda_1 = \alpha_2 = \lambda_2 = 1$ with the relaxation parameter $\theta = \frac{1}{2}$. It was also shown that the iteration then converges to the exact solution in two iterations if both domains are of the same size. In our heterogeneous case, this choice of relaxation parameter becomes $\theta = \frac{\sqrt{\alpha_2\lambda_2}}{\sqrt{\alpha_1\lambda_1}+\sqrt{\alpha_2\lambda_2}}$, and we can also obtain convergence in two iterations:

Theorem 1 *If $\sqrt{\alpha_1/\lambda_1}a = \sqrt{\alpha_2/\lambda_2}b$, the DNWR iteration converges in two iterations for $\theta = \frac{\sqrt{\alpha_2\lambda_2}}{\sqrt{\alpha_1\lambda_1}+\sqrt{\alpha_2\lambda_2}}$.*

Proof. If $\sqrt{\alpha_1/\lambda_1}a = \sqrt{\alpha_2/\lambda_2}b$, the first iterate becomes $\hat{h}^1 = \left((1-\theta) - \theta\sqrt{\frac{\alpha_1\lambda_1}{\alpha_2\lambda_2}}\right)\hat{h}^0$, which is independent of s. If $\theta = \frac{\sqrt{\alpha_2\lambda_2}}{\sqrt{\alpha_1\lambda_1}+\sqrt{\alpha_2\lambda_2}}$ then $\left((1-\theta) - \theta\sqrt{\frac{\alpha_1\lambda_1}{\alpha_2\lambda_2}}\right) = 0$. Hence the error is zero, and we have the exact solution on the interface after one iteration, and thus in the subdomains after two iterations. □

With $\theta = \frac{\sqrt{\alpha_2\lambda_2}}{\sqrt{\alpha_1\lambda_1}+\sqrt{\alpha_2\lambda_2}}$ as in Theorem 1, we can also obtain linear and super-linear convergence estimates in the case when $\sqrt{\alpha_1/\lambda_1}a \neq \sqrt{\alpha_2/\lambda_2}b$. The update (5) in the DNWR iteration then becomes

$$\hat{h}^k = \left(- \frac{\sqrt{\alpha_1\lambda_1}}{\sqrt{\alpha_2\lambda_2}+\sqrt{\alpha_1\lambda_1}} \frac{\sinh((\sqrt{\alpha_2/\lambda_2}b - \sqrt{\alpha_1/\lambda_1}a)\sqrt{s})}{\sinh(\sqrt{\alpha_1/\lambda_1}a\sqrt{s})\cosh(\sqrt{\alpha_2/\lambda_2}b\sqrt{s})} \right)^k \hat{h}^0. \quad (6)$$

In order to derive these convergence estimates, we use kernel estimates from [5, Theorem 2] and [3, Lemma 3.1 and 3.3], which we summarize as follows:

Lemma 1 *For $\alpha > 0 \in \mathbb{R}$, $\beta > 0 \in \mathbb{R}$ and $h \in L^\infty(0,\infty)$ we have on the time interval $[0,T]$ for all T including infinity the linear kernel estimate*

$$\left\| \mathcal{L}^{-1}\left(\left(\frac{\sinh\left((\beta-\alpha)\sqrt{s}\right)}{\sinh\left(\alpha\sqrt{s}\right)\cosh\left(\beta\sqrt{s}\right)} \right)^k \hat{h} \right) \right\|_\infty \leq \left(\frac{|\alpha-\beta|}{\alpha} \right)^k \|h\|_\infty ,$$

where $\mathcal{L}^{-1}$ denotes the inverse Laplace transform and s the Laplace variable.

Lemma 2 *For $\alpha > 0 \in \mathbb{R}$, $\beta > 0 \in \mathbb{R}$ and $h \in L^\infty(0,T)$ we have two super-linear kernel estimates on the bounded time interval $[0,T]$: if $\alpha > \beta$, then*

$$\left\| \mathcal{L}^{-1}\left(\left(\frac{\sinh\left((\beta-\alpha)\sqrt{s}\right)}{\sinh\left(\alpha\sqrt{s}\right)\cosh\left(\beta\sqrt{s}\right)} \right)^k \hat{h} \right) \right\|_\infty \leq 2^k \left(\frac{\alpha-\beta}{\alpha} \right)^k erfc\left(\frac{k\beta}{2\sqrt{T}} \right) \|h\|_\infty ,$$

where $erfc(t) = \frac{2}{\sqrt{\pi}} \int_t^\infty e^{-\tau^2} d\tau$. If $\alpha < \beta$ we have instead

$$\left\| \mathcal{L}^{-1}\left(\left(\frac{\sinh\left((\beta-\alpha)\sqrt{s}\right)}{\sinh\left(a\sqrt{s}\right)\cosh\left(\beta\sqrt{s}\right)} \right)^{2k} \hat{h} \right) \right\|_\infty \leq \left(\frac{2\sqrt{2}}{1-\exp\left(-\frac{(2k+1)\alpha^2}{T}\right)} \right)^{2k} \exp\left(\frac{-k^2\alpha^2}{T} \right) \|h\|_\infty .$$

We can now state and proof our new linear and super-linear convergence estimates for the heterogeneous DNWR iteration (2)–(3).

Theorem 2 (Linear estimate on unbounded time intervals) *If $\sqrt{\alpha_1/\lambda_1}a \neq \sqrt{\alpha_2/\lambda_2}b$ and $\theta = \frac{\sqrt{\alpha_2\lambda_2}}{\sqrt{\alpha_1\lambda_1}+\sqrt{\alpha_2\lambda_2}}$, then the error of the heterogeneous DNWR iteration (2)–(3) on the time interval $[0,T]$, where T can be infinite, satisfies the linear convergence estimate*

$$||h^k||_\infty \leq \left(\frac{\left|1 - \frac{\sqrt{\alpha_2\lambda_1}b}{\sqrt{\alpha_1\lambda_2}a}\right|}{1+\sqrt{\frac{\alpha_2\lambda_2}{\alpha_1\lambda_1}}} \right)^k ||h^0||_\infty .$$

Proof. Applying the linear kernel estimate from Lemma 1 with $\alpha = \sqrt{\frac{\alpha_1}{\lambda_1}}a$ and $\beta = \sqrt{\frac{\alpha_2}{\lambda_2}}b$ yields

$$\left\|h^k\right\|_\infty \leq \left(\frac{\sqrt{\alpha_1\lambda_1}}{\sqrt{\alpha_2\lambda_2}+\sqrt{\alpha_1\lambda_1}}\right)^k \left(\frac{\left|\sqrt{\frac{\alpha_2}{\lambda_2}}b-\sqrt{\frac{\alpha_1}{\lambda_1}}a\right|}{\sqrt{\frac{\alpha_1}{\lambda_1}}a}\right)^k \left\|h^0\right\|_\infty = \left(\frac{\left|1-\frac{\sqrt{\alpha_2\lambda_1}b}{\sqrt{\alpha_1\lambda_2}a}\right|}{1+\sqrt{\frac{\alpha_2\lambda_2}{\alpha_1\lambda_1}}}\right)^k \left\|h^0\right\|_\infty$$

which concludes the proof. □

Theorem 3 (Superlinear estimate on bounded time intervals) *Let* $\theta = \frac{\sqrt{\alpha_2\lambda_2}}{\sqrt{\alpha_1\lambda_1}+\sqrt{\alpha_2\lambda_2}}$. *If* $\sqrt{\alpha_1/\lambda_1}a > \sqrt{\alpha_2/\lambda_2}b$, *then the heterogeneous DNWR iteration* (2)–(3) *satisfies on the bounded time interval* $[0,T]$ *the super-linear convergence estimate*

$$\left\|h^k\right\|_\infty \leq \left(2\frac{1-\frac{\sqrt{\alpha_2\lambda_1}b}{\sqrt{\alpha_1\lambda_2}a}}{1+\sqrt{\frac{\alpha_2\lambda_2}{\alpha_1\lambda_1}}}\right)^k erfc\left(\frac{k}{2}\sqrt{\frac{\alpha_2}{\lambda_2 T}}b\right)\left\|h^0\right\|_\infty.$$

If $\sqrt{\alpha_1/\lambda_1}a < \sqrt{\alpha_2/\lambda_2}b$, *then we have instead*

$$\left\|h^{2k}\right\|_\infty \leq \left(\frac{2\sqrt{2}}{\left(1+\sqrt{\frac{\alpha_2\lambda_2}{\alpha_1\lambda_1}}\right)\left(1-\exp\left(\frac{-(2k+1)\alpha_1a^2}{\lambda_1 T}\right)\right)}\right)^{2k} \exp\left(\frac{-k^2\alpha_1a^2}{\lambda_1 T}\right)\left\|h^0\right\|_\infty.$$

Proof. Using the super-linear kernel estimate for the case $\alpha > \beta$ in Lemma 2 with $\alpha = \sqrt{\alpha_1/\lambda_1}a$ and $\beta = \sqrt{\alpha_2/\lambda_2}b$ yields directly

$$\left\|\mathcal{L}^{-1}\left(\hat{h}^k\right)\right\|_\infty \leq \left(2\frac{1-\frac{\sqrt{\alpha_2\lambda_1}b}{\sqrt{\alpha_1\lambda_2}a}}{1+\sqrt{\frac{\alpha_2\lambda_2}{\alpha_1\lambda_1}}}\right)^k \operatorname{erfc}\left(\frac{k}{2}\sqrt{\frac{\alpha_2}{\lambda_2 T}}b\right).$$

For the other case where $\sqrt{\alpha_1/\lambda_1}a < \sqrt{\alpha_2/\lambda_2}b$, we can instead use the super-linear kernel estimate for $\alpha < \beta$ with $\alpha = \sqrt{\alpha_1/\lambda_1}a$ and $\beta = \sqrt{\alpha_2/\lambda_2}b$ yielding

$$\left\|h^{2k}\right\|_\infty \leq \left(\frac{2\sqrt{2}}{\left(1+\frac{\sqrt{\alpha_2\lambda_2}}{\sqrt{\alpha_1\lambda_1}}\right)\left(1-\exp(\frac{-(2k+1)a^2\alpha_1}{\lambda_1 T})\right)}\right)^{2k} \exp\left(\frac{-k^2\alpha_1a^2}{\lambda_1 T}\right)\left\|h^0\right\|_\infty.$$

□

Note that the linear convergence estimate in Theorem 2 can be bigger than one, and hence the estimate does not always guarantee convergence. This is for example the case if the ratio α_1/α_2 is large and λ_1/λ_2 is small. Similarly, the linear estimate will yield fast convergence if the ratios α_1/α_2 and λ_1/λ_2 are both small. This shows that the domain ordering has a big impact on the linear convergence estimate if there is a big jump in material parameters or domain sizes.

This is in contrast to the super-linear convergence estimate in Theorem 3, which guarantees convergence for all parameter combinations. Note also that the super-

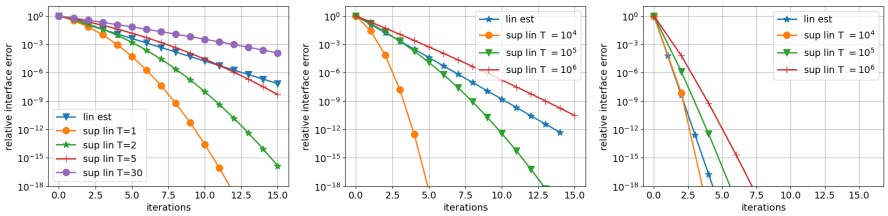

Fig. 1: The linear and super-linear error bounds for the simple test case (left), and the two realistic material combinations steel-air and air-steel (middle and right).

linear convergence estimate predicts faster convergence, the larger $\sqrt{\alpha_1/\lambda_1}a/\sqrt{T}$ and $\sqrt{\alpha_2/\lambda_2}b/\sqrt{T}$ are. More importantly both factors increase when T decreases, suggesting that splitting the simulation time T into multiple smaller time windows improves the convergence speed.

3 Numerical Experiments

In this section we now study numerically how sharp the linear and super-linear error bounds from Theorem 2 and 3 are. We use first a simple test case, where all parameters including the domain sizes are equal to 1 except for $\alpha_1 = 4$, and then also a more advanced test case with realistic parameters for air and steel which also was used in [7]. We still use domain length one, but the material parameters for air are $\alpha = 1299$, $\lambda = 0.0243$, and for steel $\alpha = 3.47 \cdot 10^6$, $\lambda = 48.9$. For reference, the factor $\sqrt{\frac{\alpha}{\lambda}}$ is 231 for air and 266 for steel. We would thus expect that the magnitude of T where we see a transition to super-linear convergence increases by a factor of 10^4 compared to our simple test case. The air and steel domains can then be combined in the two configurations air-steel or steel-air, depending on whether the air or steel domain has the Dirichlet transmission condition.

We show the linear and super-linear error bounds for all cases in Figure 1 for different iteration numbers and simulation times. For the simple test case, and the simulation time $T < 2$, we see that the super-linear error bound is tighter than the linear error bound for all iterations. We can thus expect that the DNWR iteration converges super-linearly in this case. The linear error bound is however tighter for the first 10 iterations for $T = 5$, and for the first 15 iterations for $T = 30$.

For the two test cases with realistic parameters, we observe a similar trend when T increases. The magnitude of T where we see a transition to super-linear convergence has increased by a factor of 10^4, demonstrating that the factor $\sqrt{\frac{\alpha}{\lambda}}$ is a good indicator for the super linear convergence regime. Furthermore, the material combination steel-air is predicted by our analysis to converge much faster than air-steel, indicating that the choice of Dirichlet domain can have a big influence on the convergence speed, consistent with observations in [7].

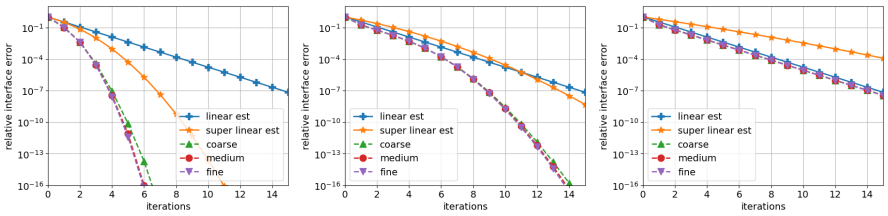

Fig. 2: The relative error on the interface compared to the linear and super-linear error bounds for the simple test case. From left to right with $T = 1, 5, 30$.

To test this in a numerical setting, we discretize the error equations for our test cases with a second order linear finite element method in space and Backward Euler in time, see [6] for details. We choose a random initial guess h^0 to test the algorithm, for the importance of this, see [2, Section 5.1]. To also see the influence of the discretization, we use a fine, medium and coarse discretization, which for the simple test case is $\Delta x = 1 \cdot 10^{-3}, 2 \cdot 10^{-3}, 4 \cdot 10^{-3}$ and $\Delta t = 10^{-3}, 4 \cdot 10^{-3}, 16 \cdot 10^{-3}$, and for the realistic test case $\Delta x = 1 \cdot 10^{-3}, 2 \cdot 10^{-3}, 4 \cdot 10^{-3}$ and $\Delta t = 20, 80, 320$, both chosen to be in the PDE convergence regime.

We show in Figure 2 the relative interface error given by $||x^k||_\infty / ||x^0||_\infty$ for the simple test case for the simulation times $T = 1$, 5 and 30. We see on the right that the linear error bound is quite sharp for the large simulation time $T = 30$, and the DNWR algorithm is in its linear convergence regime. For $T = 5$ in the middle in Figure 2, the linear estimate is still sharp for the first few iterations, but then the DNWR algorithm transits into its super-linear convergence regime. We see that the super-linear convergence estimate is not as sharp as the linear one, but it still indicates that the algorithm must go into the super-linear convergence regime at some point by becoming smaller than the linear bound. For short times, $T = 1$ in Figure 2 on the left, the super-linear error bound is tighter than the linear error bound, and indeed the DNWR algorithm converges right from the start super-linearly. Again, however, the super-linear estimate is not quite sharp.

The corresponding results for the realistic test case for $T = 10^4$, 10^5 and 10^6, are shown in in Figure 3, both for the good and bad assignment of the Dirichlet transmission condition.

We see a similar transition from the super-linear to the linear regime when T increases. In all cases the air-steel test case achieves faster convergence speeds showing that the domain configuration matters, and our new theoretical results allow us to make a good choice in advance. However, the steel-air case still reaches an error of 10^{-13} for $T = 10^4$ in 3 iterations indicating that we see fast convergence even with a bad domain configuration if the simulation time is kept short enough, and this is again predicted by our theoretical results.

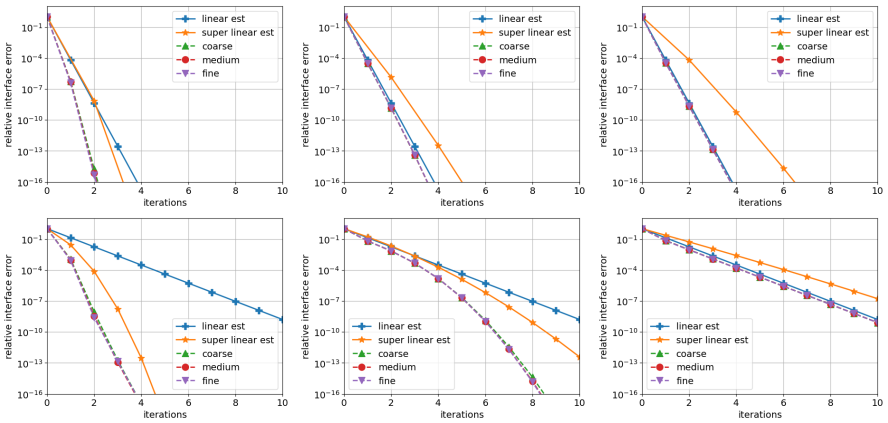

Fig. 3: The relative error on the interface compared to the linear and super-linear error bounds for the air-steel case in the top row and steel-air case in the bottom row. From left to right with $T = 10^4, 10^5$ and 10^6.

4 Conclusion

We derived new error bounds for DNWR to solve heterogeneous 1D heat equations. These bounds allow us to decide in advance which subdomain should use the Dirichlet transmission condition for best performance. Our numerical experiments show that the linear error bound is sharp for long time windows, and that the super-linear error bound still describes qualitatively well convergence for short time windows.

References

1. S. Clement, F. Lemarié, and E. Blayo, *Discrete analysis of Schwarz waveform relaxation for a diffusion reaction problem with discontinuous coefficients*, SMAI J. Comp. Math., 8 (2022), pp. 99–124.
2. M. J. Gander, *Schwarz methods over the course of time*, Electron. Trans. Numer. Anal, 31 (2008), pp. 228–255.
3. M. J. Gander, F. Kwok, and B. C. Mandal, *Dirichlet-Neumann and Neumann-Neumann waveform relaxation algorithms for parabolic problems*, ETNA, 45 (2016), pp. 424–456.
4. F. Lemarié, L. Debreu, and E. Blayo, *Toward an optimized global-in-time Schwarz algorithm for diffusion equations with discontinuous and spatially variable coefficients. Part 1: the constant coefficients case*, ETNA, 40 (2013), pp. 148–169.
5. M. Mandal, *A time-dependent Dirichlet-Neumann method for the heat equation*, Domain Decomposition Methods in Science and Engineering XXI, (2013), pp. 467–475.
6. P. Meisrimel, A. Monge, and P. Birken, *A time adaptive multirate Dirichlet–Neumann waveform relaxation method for heterogeneous coupled heat equations*, ZAMM, 103 (2023).
7. A. Monge and P. Birken, *On the convergence rate of the Dirichlet–Neumann iteration for unsteady thermal fluid–structure interaction*, Computational Mechanics, 62 (2018), pp. 525–541.